Brane parity orders in the insulating state of Hubbard ladders

Brane parity orders in the insulating state of Hubbard ladders

Cristian Degli Esposti Boschi,[1] Arianna Montorsi,[2] and Marco Roncaglia[2]
[1]*CNR-IMM, Sezione di Bologna, I-40129, Italy*
[2]*Institute for Condensed Matter Physics and Complex Systems, DISAT, Politecnico di Torino, I-10129, Italy*
(Received 17 December 2015; revised manuscript received 7 July 2016; published 11 August 2016)

The Mott insulating state of the Hubbard model at half filling could be depicted as a spin liquid of singly occupied sites with holon-doublon quantum fluctuations localized in pairs. In one dimension the behavior is captured by a finite value of the charge parity string correlator, which fails to remain finite when generalized to higher dimensions. We recover a definition of parity brane correlator which may remain nonvanishing in the presence of interchain coupling, by assigning an appropriate fractional phase to the parity breaking fluctuations. In the case of Hubbard ladders at half filling, we find that the charge parity brane is nonzero at any repulsive value of interaction. The spin-parity brane instead becomes nonvanishing in the even-leg case, in correspondence to the onset of the spin gapped D-Mott phase, which is absent in the odd-leg case. The behavior of the parity correlators is also analyzed by means of a numerical DMRG analysis of the one- and two-leg ladder.

DOI: 10.1103/PhysRevB.94.085119

I. INTRODUCTION

The presence of nonlocal orders (NLO) in various low temperature phases of quantum matter, ultimately relying on entanglement of short/long-range degrees of freedom, is a fascinating theoretical prediction [1] which has recently also been observed in experimental settings [2,3]. NLO amount to the nonvanishing expectation value of correlators between nonlocal operators. The fact seems to contradict Landau's paradigm, which associates the formation of ordered phases to the breaking in the ground state of some symmetries of the Hamiltonian and to the corresponding finite asymptotic value of appropriate correlators between local observables, identified as order parameters. NLO connect with the presence of topological orders, which has been thoroughly investigated in the past two decades since their identification in edge states of fractional quantum Hall liquids [4], to the recent classification of topological phases of noninteracting fermions [5]. In case of quantum chains of interacting spins, general results have been achieved for one-dimensional systems [6,7], introducing the concept of symmetry protected topological (SPT) phases. These have been subsequently extended to interacting fermionic systems [8] (see also [9] for a review).

Nonlocal correlators appear to play the role of order parameters for SPT phases [10,11]. However, phases with NLO may be trivial from the point of view of topological order: this is the case for instance for the Mott insulator (MI) in the one-dimensional (1D) Hubbard model, characterized by a nonvanishing value of the charge parity correlator in the asysmptotic limit, both in the bosonic [12] and in the fermionic case [13]. The 1D parity correlator is the string product of site parities connecting two arbitrary points in the lattice. More generally, a bosonization analysis has proved that NLO configure as order parameters for the ordered phases of spinful fermions in 1D with time reversal symmetry: each pinned value of either the spin or charge bosonic fields corresponds to the presence of specific nonvanishing NLO [14], a fact that suggests a possible fundamental role of NLO in fermionic systems. Also, since string correlators are products of quantities on physical sites, they can be easily measured in experimental setups on optical lattices, representing a feasible way to distinguish phases with and without topological order [15].

The generalization of the above concepts to higher dimension is not straightforward. It has been argued that string orders and SPT phases are fragile with respect to interchain tunneling [16–18], when the system breaks reflection symmetry. Even in the presence of such symmetry, in [17] it was shown that stringlike correlations decay to zero with an area law in the two-dimensional (2D) case: the proof holds for correlators between points. A different definition of the parity correlator in two dimensions [19] relies instead on a generalization of string to branes when moving to 2D systems. In this case the parity correlator was shown to exhibit a "perimeter law" decay to zero within the MI phase.

While some specific definition of nonlocal order may be evanescent in higher dimension, the underlying physics could persist in appropriate phases [12,20]. In the case of parity, it is related to the presence of finite-size localized pairs of parity-changing objects which as a whole do not destroy the parity of the background. The characterization of such behavior by means of observables, as well as its identification in appropriate physical systems, is a relevant open issue.

II. FRACTIONAL PARITY BRANES

Here we revisit the definition of NLO, by specializing to parity orders, with the scope of capturing their role in the onset of insulating behavior in higher dimension. We focus on the 2D fermionic case, though most of the concepts introduced can be easily generalized to higher dimension. According to the analysis developed in [13], at least two types of parity correlators can be identified in these systems, thanks to the conservation of both charge and spin. We adapt to spin and charge parity correlators a definition first introduced in [21] for detecting Haldane-type orders. This amounts to considering in 2D branes of operators bounded by rungs rather than 1D strings bounded by sites, at the same time assigning a phase term $\exp(i\theta)$ to the parity-destroying elements. Here by 2D branes we mean a connected region of the infinite plane, delimited by a well-defined perimeter. In the specific ladder case considered in the following, we look at a portion of the ladder delimited by

two rungs: the 2D limit is recovered by increasing their length, i.e., the number of legs. We show that θ should be scaled down with that number, in order to capture the presence of parity order in the corresponding gapped phases. We then adopt the definition of such nonlocal fractional parity brane correlators to the study at half filling of the repulsive Hubbard model on a chain and a two-leg ladder.

A. Definition

We think of a $M \times N$ lattice as a N-rung, M-leg ladder. The lattice is folded onto a torus by assuming periodic boundary conditions (PBC) in both directions. The total Hilbert space is the direct product $\mathcal{H} = \bigotimes_k \mathcal{H}_k$ of local Hilbert spaces $\mathcal{H}_k$ defined on the rungs ($k = 1, \ldots, N$). In general, each symmetry of the model Hamiltonian can be decomposed into irreducible representations with well defined Cartan generators. Let us focus on a specific local Cartan generator h_k with highest weight Λ. We define the parity string operators

$$O_P^{(h)}(j) = \prod_{k<j} \exp\left(i\pi \frac{h_k}{\Lambda}\right). \tag{1}$$

In case it is nonzero, the local operator h_k assumes $2\Lambda + 1$ discrete values in the interval $-\Lambda \leqslant h_k \leqslant \Lambda$. We now introduce the string correlators

$$\mathcal{C}_P^{(h)}(r) = \langle O^{(h)\dagger}(j) O^{(h)}(j+r) \rangle, \tag{2}$$

and we say that we are in the presence of parity hidden order when $\mathcal{C}_P{}^{(h)}(r)$ is nonvanishing in the limit $r \to \infty$. It is important to notice that in our definition (1) the eigenvalues of the Cartan generators in the local representation have been renormalized by Λ, so that the phase factor in the exponent varies in the interval $[-\pi,\pi]$. This choice is crucial to avoid unwanted phase cancellations along the rungs that would come up without the division by Λ in Eq. (1), especially when the rung size M is increased and accordingly also Λ grows (depending on the irrep we are considering). Our choice is at odds with a majority of the string operators studied in the recent literature (see for instance [19]) though consistent with some previous literature on spin systems, like Ref. [21] where a Haldane string of spins ($h_k = S_k^z$, in that case) was studied in a two-leg ladder. As an example which we will thoroughly discuss, in the fermionic Hubbard chain with charge and spin conservation $\mathcal{C}_P^{(h)}(r)$ coincides with the so-called parity correlators [2,13], with k single site index, $h_k \equiv S_{\nu k}^z$, $\nu = c,s$, and $S_{ck}^z = (n_{k\uparrow} + n_{k\downarrow} - 1)/2$, $S_{sk}^z = (n_{k\uparrow} - n_{k\downarrow})/2$ the pseudospin and spin operator, respectively, and, of course, $\Lambda = 1/2$.

The definition (1) is decisive for the persistence of string order when we consider the 2D limit $M \to \infty$

$$\mathcal{C}_P(h) \doteq \lim_{M\to\infty} \lim_{r\to\infty} \mathcal{C}_P^{(h_M)}(r), \tag{3}$$

where h_M is a Cartan generator of the symmetry algebra of the Hamiltonian model for a rung of length M. In the following section we give some arguments to support our choice.

B. Diluted empty-doublon pairs limit

Close to the atomic limit, approached for large interactions, we can consider empty-doublon fluctuations as dilute and independent. Let us consider a domain limited by two rungs of total length $2M$. Paired fluctuations that lie entirely inside or outside such a domain do not contribute to a phase term in Eq. (1). The terms that are candidates to destroy the parity order are given by pairs where one partner lies inside the domain, while the other is outside. A schematic representation of this construction is given in Fig. 1. In the standard parity order, every "cut" gives a -1, so the parity order is given by the difference of all the configurations with an even number of cuts minus all the configurations with an odd number. A probability calculation [20] that assumes all the configurations equally probable (dilution limit) shows that the parity order vanishes with M, with a "perimeter law."

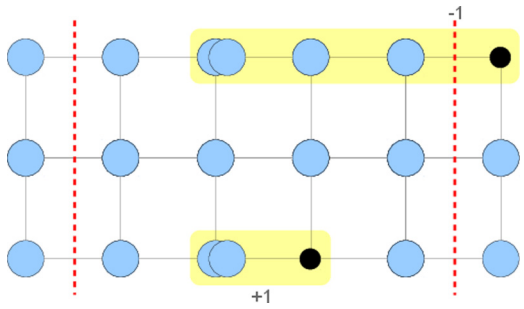

FIG. 1. Schematic representation of a three-leg ($M = 3$) ladder with nearest neighbor connections. In this configuration blue circles indicate lattice sites with one fermion, black dots indicate empty sites, and superimposed circles are double occupied sites. In a state with total null magnetization the latter form pairs represented by yellow bounded regions, in a notation similar to that of Ref. [20]. Red dashed lines are the vertical boundaries of an area on which the parity correlators are computed; in standard parity order every time that a pairing path cuts the boundary one collects a factor (-1), that is absent when the path is fully inside the area.

On the contrary, we show that the parity correlator defined in Eq. (1) remains finite in the gapped phase. In fact, let's confine our analysis to a symmetry algebra $su(2\nu)$ (ν positive integer): when we consider the rung pseudospin $S_\nu^z(j) = \sum_{l=1}^M S_\nu^z(j,l)$ (l site and j rung index), we recognize that in this case the highest weight is $\Lambda = M/2$. The fractional parity operators (1) become

$$O_P^{(\nu)}(j) = \prod_{k<j} \exp\left[i\frac{2\pi}{M} S_\nu^z(j)\right]. \tag{4}$$

With a similar probability argument as the one proposed in [20], we assign a probability p to find a broken pair in correspondence of each lattice site along the boundary. In particular, if the partner inside the domain is an empty site, the contribution is $\exp(-i\frac{\pi}{M})$; if instead the doublon is inside the contribution is $\exp(i\frac{\pi}{M})$. A probability calculation gives a two-point (-rung) correlator (2)

$$\mathcal{C}_P^{(\nu)}(r) = \left[1 - p\left(1 - \cos\frac{\pi}{M}\right)\right]^{2M}, \tag{5}$$

where the separation r is larger than the typical size of the disordering pairs. Interestingly Eq. (5) tends to 1 in the limit $M \to \infty$. This promotes the 2D fractional parity correlator (3) as a good order parameter to remain finite in the MI phase.

In case the rungs are uncorrelated, the same reasoning of the previous paragraph shows that $\mathcal{C}_P(r) = [1 - p(1 - \cos\frac{\pi}{M})]^{MN}$, which, upon considering the limit in the order as in Eq. (3), correctly reproduces a vanishing value for the 2D brane correlator. In the present formulation, the qualitative result is independent of the specific 2D domain chosen: we do not necessarily deal with regions bounded by two rungs, but we can depict any collection of closed domains with perimeter $2M$. The essential fact in order to possibly get a finite fractional parity is that the "cut" disordering pairs must be localized along the perimeter.

III. HUBBARD MODEL AT HALF FILLING ON A LADDER

The model Hamiltonian reads

$$H_{\rm Hub} = -\sum_{\langle i,j\rangle\sigma} c^\dagger_{i\sigma} c_{j\sigma} + U \sum_i \left(n_{i\uparrow} - \frac{1}{2}\right)\left(n_{i\downarrow} - \frac{1}{2}\right),$$

where $c_{i\sigma}$ indicates a fermionic annihilation operator with spin σ at site i, and $n_{i\sigma} = c^\dagger_{i\sigma} c_{i\sigma}$ is the associated number operator.

At half filling the symmetry algebra of the Hamiltonian, induced by total spin and pseudospin conservation, is $su(2) \bigoplus su(2)$ [22]. The symmetry algebra has charge and spin Cartan operators, namely $S^z_\nu = \sum_j S^z_{\nu j}$, with $\nu = c,s$, respectively (see also Sec. II A).

For an infinite value of particle interaction U, the ground state of the half filled fermionic (and bosonic) Hubbard model displays a MI phase in the repulsive case, where each site contains exactly one particle, and parity order is equal to unity in the charge sector. For large enough positive values of the interaction, the MI phase is also characterized by holon-doublon quantum fluctuations, which remain confined in the background of singly occupied sites. This can be seen for instance through the strong coupling $\frac{t}{U}$ expansion of the Hubbard Hamiltonan [23], leading to second order to the Heisenberg Hamiltonian: each even order $2l$ introduces in the infinite U ground state l holon-doublon virtual pairs of size at most equal to l. In the attractive interaction case, at zero magnetization and arbitrary filling, a specular description should hold by interchanging holon-doublon and up-down spin single particle roles.

For the 1D chain, the parity order in the charge sector (which assigns the minus sign to both holons and doublons) remains asymptotically finite in the MI phase and vanishes at $U = 0$ [13]. Whereas in the spin sector the spin-parity order is vanishing in the MI phase and becomes finite for negative U. The system enters a Luther Emery liquid (LE) phase: each site contains either holons or doublons, with quantum fluctuations of single electrons with up and down spins [13]. In 2D, the system in the repulsive case is expected to be an antiferromagnetic insulator with vanishing spin gap. The "paired fluctuation" physical picture of the insulator should still hold [20,23]. However, up to now the proposed 2D generalizations of the parity correlator have failed to remain finite in the corresponding phases.

In this section, we apply the definition of spin- and charge parity orders introduced in the previous section to investigate, both by bosonization and numerical analysis, their behavior in the repulsive regime of the Hubbard model on ladders.

A. Bosonization analysis of repulsive M-leg ladder

The bosonization analysis of the Hubbard model on a ladder at half filling was first considered in the weak coupling limit in the two-leg case [24,25], and extended to the generalized Hubbard model case in [26,27]. At variance with the single chain case, for repulsive values of the interaction the insulating phase is fully gapped: also the spin liquid becomes insulating, and the phase is denoted as D-Mott. The bosonization analysis was successively extended to the M-leg case in [28] and [29]. The analysis in the weakly interacting repulsive case shows an even-odd effect. At appropriate energy scales, for M even the Hamiltonian becomes the sum of $M/2$ decoupled two-leg ladder Hamiltonians, whereas for M odd it is the sum of $(M-1)/2$ two-leg ladder plus a single chain Hamiltonian. Thus the behavior of the M-leg ladder can be derived from that of the single- and two-chain cases. In particular, below we will refer to the total charge and spin fields on the two-leg ladder as ϕ^+_ν, and on the single chain as $\sqrt{2}\phi_\nu$: according to the literature [30,31], in the charge sector they both are locked to the value zero (modulo integer multiples of π), whereas in the spin sector ϕ^+_s is locked to the value zero, while $\sqrt{2}\phi_s$ is unpinned. So that the total charge field is always pinned to zero, the total spin field in the even M case is pinned to zero, giving rise to a D-Mott phase, but in the odd M case it is unpinned, recovering the 1D-like spin liquid MI. Depending on the strength of interaction, a dimensional crossover is also expected with increasing the number of legs, signaled by the suppression of the spin gap also in the even leg case, and to the collapse to the antiferromagnetic insulating phase characteristic of the 2D system.

We now proceed to investigate how the above features reflect into the values of the charge and the spin brane parity correlators introduced in the previous section. Within the bosonization approach, the parity correlators can be evaluated by noticing that the product of the exponentials in Eq. (1) in the continuum limit becomes the exponential of the integral along the rung chain of $2\pi S^z_\nu(x)$, with the total rung densities $S^z_\nu(x) \doteq \frac{1}{M}\sum_l S^z_\nu(x,l)$ ($\nu = c,s$, respectively). Due to the paired chain structure of the bosonized problem, we can assume $S^z_\nu(x) \approx \frac{1}{2}([S^z_\nu(x,1) + S^z_\nu(x,2)] \doteq \frac{1}{2\pi}\partial_x\phi^+_\nu$ for even M; and, analogously, $S^z_\nu(x) \approx \frac{1}{2\pi M}[(M-1)\partial_x\phi^+_\nu + \sqrt{2}\partial_x\phi_\nu]$, for odd M. So that, exploiting the particle-hole symmetry, one has

$$O^\nu_P(x) \approx \cos\tilde{\phi}_\nu(x),$$

with $\tilde{\phi}_\nu \equiv \phi^+_\nu$ for M even, and $\tilde{\phi}_\nu \equiv \phi^+_\nu + \frac{1}{M}(\phi_\nu - \phi^+_\nu)$ for M odd. The asymptotic parity correlators defined in (2) can now be evaluated according to the analysis outlined in [30] and [31] (see also [13]). In full analogy with the one-chain leg, one obtains

$$\mathcal{C}^{(\nu)}_P(r) = \langle\cos\tilde{\phi}_\nu(0)\cos\tilde{\phi}_\nu(r)\rangle.$$

When both total charge and spin bosonic fields are locked to the value zero, as in the even-leg ladder case, the corresponding brane correlators $\mathcal{C}^{(\nu)}_P$ defined in (3) become nonvanishing, signaling the simultaneous presence of two types of hidden orders: localized holon-doublon pairs, and localized up-down spin pairs. Whereas, when a single one-chain field is unlocked, also the associated total field becomes unpinned, and the corresponding correlator will have vanishing average. This is the case for the spin field in the odd-leg ladder case.

B. Numerical analysis of Hubbard chain and two-leg ladder

We now proceed to the evaluation of the brane parity spin and charge correlators, $\mathcal{C}_P^{(\nu)}(r)$ for $\nu = s,c$ and $M = 1,2$, with a series of density-matrix renormalization group (DMRG) calculations (see the Appendix for further details). Note that as long as one uses a "nonfractional" expression as in Ref. [19] for the single-site single-species operators we have $\exp(\mathrm{i}\pi n_{i\sigma}) = \exp(-\mathrm{i}\pi n_{i\sigma})$ so we will report only the charge case because the spin case is simply related to the former. At variance with the case $M = 1$ [13], the spatial dependence of the nonlocal parity correlation functions is not simply given by a decay with the distance and even-odd oscillations, but depends in a nontrivial fashion on the number of rungs and on the actual value of the interaction. After a more detailed discussion found in the Appendix here we give conventionally the values computed with open boundary conditions (OBC) from 1/4 to 3/4 of the total ladder length in terms of rungs (further averaged between the last two rungs to extract the uniform part); the choice is meant to reduce edge effects and to keep a sufficiently large distance between the rungs in the correlator.

From numerical data it is not always simple to decide whether the spin gap is open and the parity correlators vanish or not. The most delicate regime in this sense is for $U \lesssim 2$; hence we report here detailed calculations for two values of the interaction, $U = 0$ and $U = 1$. The spin gap we have considered has the usual definition $\Delta_s = E_L(N_e, S_z = 1) - E_L(N_e, S_z = 0)$, where E_L is the lowest energy eigenvalue at a given number of sites L, depending on the particle number N_e and total spin S_z. The study of Weihong and co-workers [32] at half filling puts the boundary of uncertainty about the vanishing of the spin gap close to $U = 1$ (their Fig. 6), even if it is also recalled that bosonization at half filling predicts a fully gapped system for $U > 0$. In order to inspect the behavior of the spin gap at small values of U we concentrate ourselves on the case $U = 1$ and compute Δ_s for a sequence of values of $L = 6p + 4$, $p = 1,2,\ldots,10$ and OBC (Fig. 2). This sequence is the one that gives a vanishing spin gap at finite size for half filling in the model with $U = 0$. Note that the two noninteracting bands have the form $\pm t - 2t\cos(k)$ with $k \in (0,\pi)$ in the limit $L \to \infty$, and at half filling the ground-state configuration is to fill the upper band up to $k_+ = \pi/3$ and the lower band up to $k_- = 2\pi/3$, so we can expect to have an oscillatory effect in the results for U close to or exactly zero.

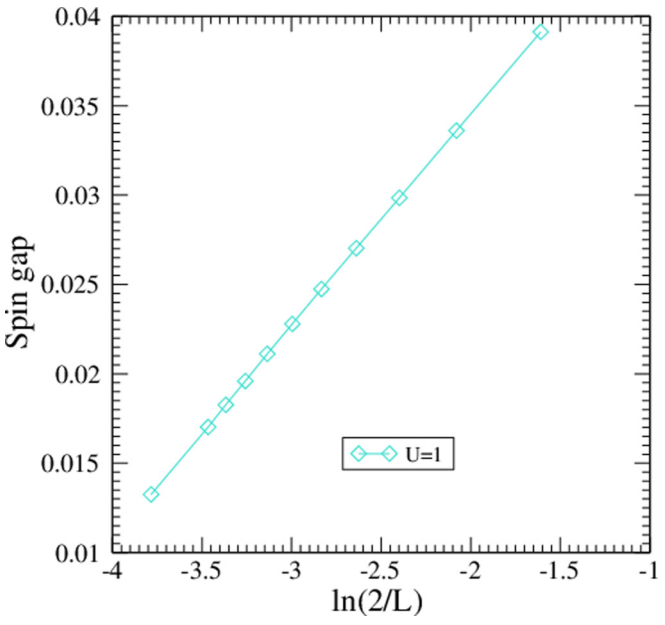

FIG. 2. Spin gap vs ladder length for $U = 1$ and OBC at half filling. The values of L are selected in such a way that the corresponding finite-size gap at $U = 0$ is null. The abscissas in this log scale suggest that at even larger sizes (left side for which the abscissas tend to $-\infty$) the data for $U = 1$ should eventually "bend up" and settle either to zero or to a small value $\lesssim O(10^{-2})$. The leftmost point corresponds to $L = 88$.

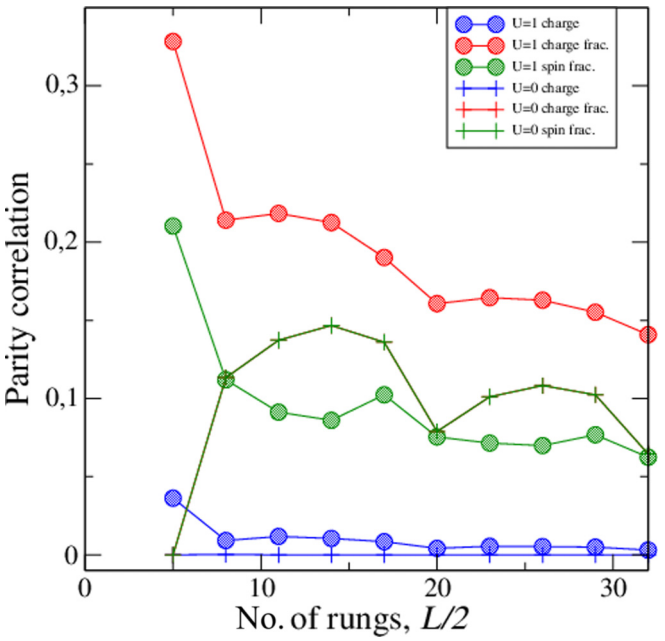

FIG. 3. Finite-size scaling of the parity correlators from one-quarter and three-quarters of the ladder length as functions of the total rung number $L/2$ for $U = 0$ and 1 (with OBC). At $U = 0$ the crosses for fractional charge and spin are almost superimposed and the nonfractional data are essentially zero. At $U = 1$ the ordering of the curves is charge fractional, spin fractional, and charge nonfractional from top to bottom.

As far as parity correlators are concerned, the results are displayed in Fig. 3 for a sequence $L = 6p + 4$ [sizes for which $\Delta_s(U = 0) = 0$ and seem to reproduce a supersequence with period 24 in L; while the values for the nonfractional parity are compatible with a vanishing value, the ones for fractional orders may eventually tend to zero but with a very slow pace. By plotting the local minima (including the data computed at $L = 88$) in log-log scale it seems (Fig. 4) that the curves for $U = 1$ show a small upward curvature, while the data for $U = 0$ (coinciding for charge and spin) scale to zero as $L^{-0.405}$.

Finally, the results at various values of U are reported in Fig. 5, where the value at $U = 0$ should be probably zero in the limit $L \to \infty$ but (as for the spin gap) we do not have a conclusive answer for $U = 1$, even if the data in Fig. 4 show a weak curvature towards positive values in this case. Notice that

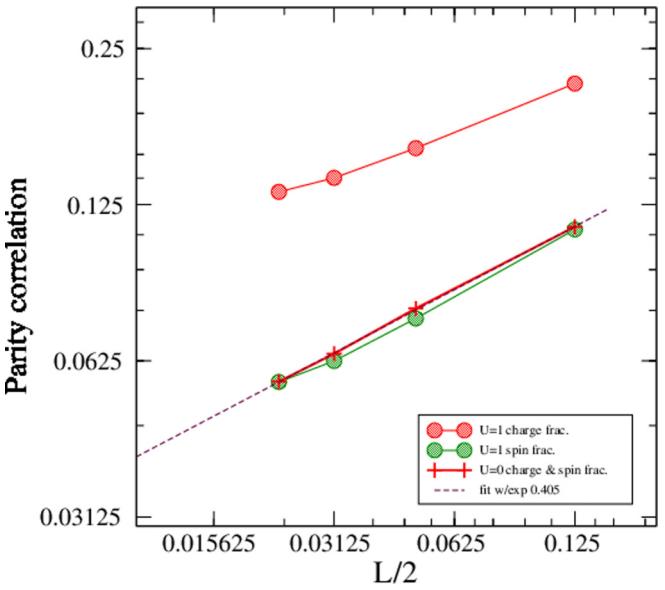

FIG. 4. As in Fig. 3 in log-log scale, including $L = 88$ with OBC. Dashed line represents a best fit for $U = 0$ data.

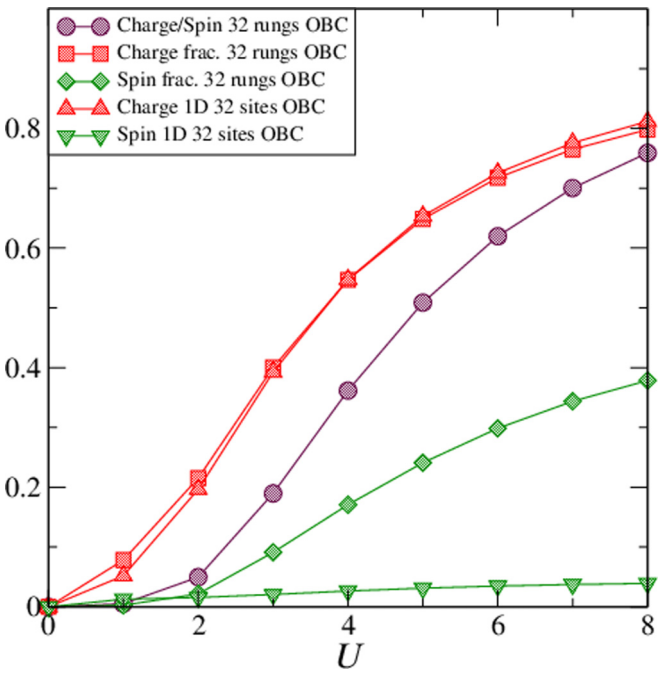

FIG. 5. Charge (red) and spin (green) fractional (squares) parity brane correlators for the two-leg ladder with OBC as functions of the repulsive interaction U, compared with the nonfractional definition (maroon circles) [19], and the one-leg ladder case (triangles). In the fractional case, increasing the number of legs, no reduction is observed for the charge parity correlator. The number of rungs (32) is expected to give a faithful picture of the thermodynamic limit for $U > 2$; finite-size effects are still present for smaller values. The plotted curves have been shifted according to the corresponding data at $U = 0$. From the arguments of Fig. 7 of the Appendix we may consider having a vanishing asymptotic value for $U = 0$ and a small finite value for $U = 1$.

in the final plot we have postprocessed the data as discussed in the Appendix, using uniform parts shifted by the finite-size values at $U = 0$ (that is, 0.04695 for $M = 1$ and 0.074892 for $M = 2$ fractional) Within the limits due to numerical errors and to the finite size (32 rungs or 32 sites in 1D), the figure clearly shows that the fractional definition of the parity brane correlators at the same time maintain constant its value in the charge sector, and passes from zero to finite in the spin sector. Whereas the nonfractional definition would exhibit a damping of the charge correlator, and an identical behavior of the spin correlator on the two-leg ladder.

IV. CONCLUSIONS

We have considered the problem of characterizing the presence and type of long range order in the Mott insulating phase of Hubbard-like models in dimension greater than 1. Our results confirm that such phase can be depicted as a spin liquid with localized correlated charge fluctuations of holons and doublons. For fermionic Hubbard models in one dimension, this behavior was already known to be captured by a nonvanishing value in the asymptotic limit of the charge parity correlator between points [13,14]. In the bosonic two-dimensional case, a recent theoretical investigation did show [19] that a parity brane correlator can be introduced, which exhibits a perimeter law decay to zero within the charge gapped phase, at variance with the area law characteristic of the gapless systems [33]. Here we proposed the fractional definition given in Eqs. (1)–(3) of the parity brane correlator on ladders, which amounts to normalize the parity to the actual length of the perimeter. We provided analytical evidence that such quantity could remain finite in two dimensions in the asymptotic limit within the insulating phase, both by investigating the strong coupling dilute limit, and through the analysis of bosonization results on ladders. We also proceeded to the numerical investigation of the single chain and two-leg ladder cases. Already in these simple cases, our definition of the charge parity correlator does not show appreciable reduction of its value with increasing the number of legs, at variance with previous ones. Moreover, by applying the same type of analysis to the fractional spin-parity brane, it is seen that the opening of the spin gap in the even legs case is signaled by its finite value, in contrast with the one-leg ladder. Noticeably, the present definition allows one to observe how charge and spin degrees of freedom could behave independently up to the 2D limit.

The results also provide a quantitative tool for detecting the occurrence of the above behavior both in experimental setups [34] and in numerical simulations of 2D systems of interacting electrons/spinful fermionic atoms. In fact, within the same framework one could also study for different parameters' regimes the possible permanence of the Luther Emery superconducting phase: by analogy with 1D findings [13], the phase may be described by a finite value of the spin-parity brane, accompanied by a vanishing value of the charge brane.

Finally, the present picture of the insulating phase of the Hubbard model can be reinterpreted in terms of entanglement and SPT phases [9]. Indeed the phase can be thought of as the infinite-U insulating phase of singly occupied sites, in which

short-range entangled pairs of holons doublons are created at finite U by appropriate local unitary transformations. This suggests a role of brane correlators as order parameters for trivial SPT phases [35] in higher dimension.

ACKNOWLEDGMENTS

A.M. acknowledges the kind hospitality of the Condensed Matter Theory Visitor's Program at Boston University, Department of Physics, as well as useful comments by Senthil Todadri. C.D.E.B. acknowledges the use of computing facilities at INFN, sezione di Bologna for a part of the DMRG calculations.

APPENDIX: DETAILS ABOUT DMRG CALCULATIONS

1. Computational parameters

In order to handle the problem $M = 2$ by means of DMRG we first have to remap it into a 1D geometry (see Fig. 6); in real space this can be done either (a) by tracing a snakelike path on the ladder or (b) by putting the two sites of a rung inside a virtual supersite with local dimension of the Hilbert space $D_{\text{rung}} = 16$ and writing all the terms of the Hamiltonian in terms of this new degree of freedom. A series of tests however indicated to us that option (b) is not convenient at all from the point of view of the computing resources to be employed, so here we present only results for option (a).

Another issue that is known to be crucial in DMRG calculations are boundary conditions and superblock geometry. While OBC (in models with nearest neighbor interactions) are usually much more favorable because in the "block+dot+dot+block" geometry a direct interaction between blocks is avoided, in this case the reordering scheme (a) above introduces block-block interactions in general, either with PBC or with the "block+dot+block+dot." However, we are interested in PBC because the core of our calculations are parity correlation functions involving a nonlocal product of operators between two "sites" of the ladder. The drawback of OBC is that there are edge effects close to the first and last sites, so in order to capture a bulk behavior of the correlation functions one has to compute them between sites that are sufficiently far from the edges. For instance, in our case we have conventionally chosen to compute the correlation functions from a starting rung at $1/4$ to $3/4$ of the total number of rungs. In this way we cover half of the ladder length, which is a meaningful distance also with PBC that on the other hand have the advantage of not involving edge effects. Moreover, the analytical results derived through bosonization formally correspond to PBC geometries. In our calculations we always fix the superblock geometry to block+dot+dot+block and perform series of similar calculations either with PBC or with OBC, in the former case "paying the price" of addtional (unavoidable) interactions between blocks. In the main text we report the data for the OBC case because they refer to larger sizes, while in this Appendix we report those for the PBC case for the sake of completeness.

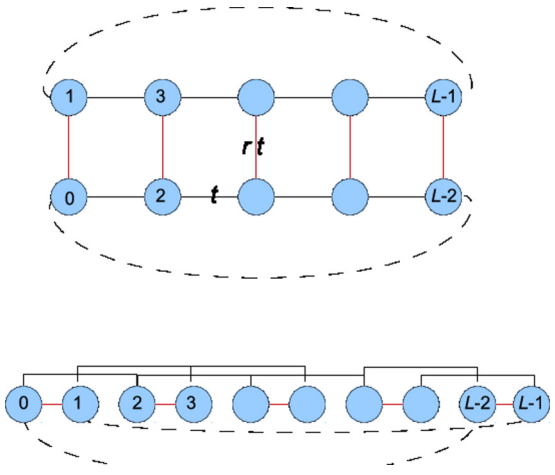

FIG. 6. Upper panel: Hubbard ladder with two legs $M = 2$. Lower panel: redistribution on a 1D chain with nearest (red) and next-to-nearest (black) neighbor couplings. The dashed lines represent the interactions to be included in case of PBC. The system has $L = N \times M$ sites in total, that is $L/2$ rungs.

As regards the number of optimized DMRG states, m_{DMRG}, an educated and conservative approach would involve an extrapolation of the results towards $m_{\text{DMRG}} \to \infty$ as, for example, in Ref. [36]. This is particularly important when phase diagrams are explored quantitatively and one wants to establish whether some specific quantity vanishes or not in the thermodynamic limit. Here, instead, due to the computational load we have decided to perform preliminary validations with up to 2048 states both for coupled and for uncoupled legs, the latter case being the most severe one for DMRG because we have essentially two interpenetrating disconnected chains. However, if not specified otherwise, the results correspond to a fixed choice of $m_{\text{DMRG}} = 1024$ states that in worst cases (half filling) yield a relative energy error of $\sim 10^{-3}$ (with respect to the exact solution obtained at $L = 16$) after five finite-system sweeps. We believe that this choice is representative, at least at a semiquantitative level, of the opening of parity orders even if the estimation of the truncation error on the latter is not trivial.

2. Parity correlators in ladders ($M = 2$)

As already evident in the 1D case in order to extract the infinite distance limit of parity correlators one has to investigate first the dependence on r. In the two-legs ladder this dependence turns out to be nontrivial and also related nonmonotonically to the system size. First we show in Fig. 7 the spatial dependence of three types of charge parity correlators, namely nonfractional (solid lines), fractional with factor $1/M = 1/2$ in the exponent (dotted lines), and nonfractional computed on the sites of a leg in the ladder (dashed lines). While the former two are symmetric with respect to the central rung in the correlator support, the latter (pointlike) decays to zero for all the values of positive U we have studied.

Moreover, Fig. 7 shows a feature that is present for all the values of U we have considered: in order to assign a finite-size value to the parity charge one cannot easily fit an infinite-distance value from the r dependence because of the nonmonotonic behavior. Hence we may conventionally fix the value at the middle of the curve, at rung number p for ladders of $4p$ or $4p + 2$ sites; in the latter case the value in the middle is typically the same on the central adjacent sites and we have noted that it acquires a small imaginary

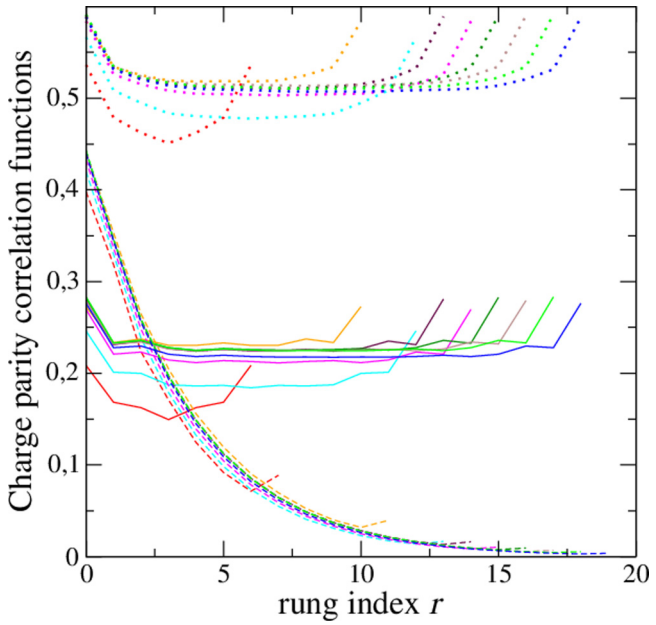

FIG. 7. Charge parity correlators as functions of the rung distance r for $U = 3$ at half filling and different systems' sizes [$L = 16$ in red, 24 in orange, 28 in cyan, 30 in maroon, 32 in magenta, 34 in dark green, 36 in brown, 38 in light green, and 40 in blue)]. Full lines indicate the nonfractional definition involving all the sites between rung 0 and rung r, while the dashed lines involve only the sites of one leg in the ladder (pointlike definition). The dotted line instead represents the brane fractional definition.

part for fractional operator. The representative central values still depend nonmonotonically on the number of sites L. In Fig. 8 we present some examples of this complex behavior for $U = 1,3,5$ to show that the finite-size sequences seem to have a regularity but with a nontrivial dependence on the

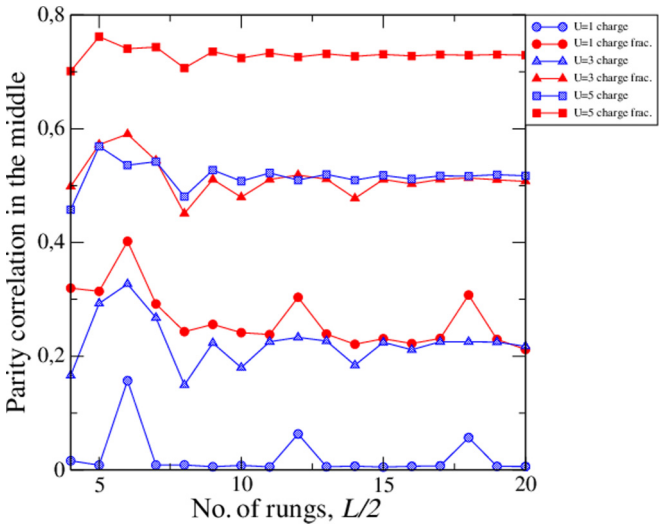

FIG. 8. Charge parity correlators in the middle of the ladder as functions of the total rung number $L/2$ for three different choices of $U = 1,3,5$ that yield different alternating behaviors (half filling). Shaded blue symbols represent nonfractional charge parity, while full red symbols represent the fractional version.

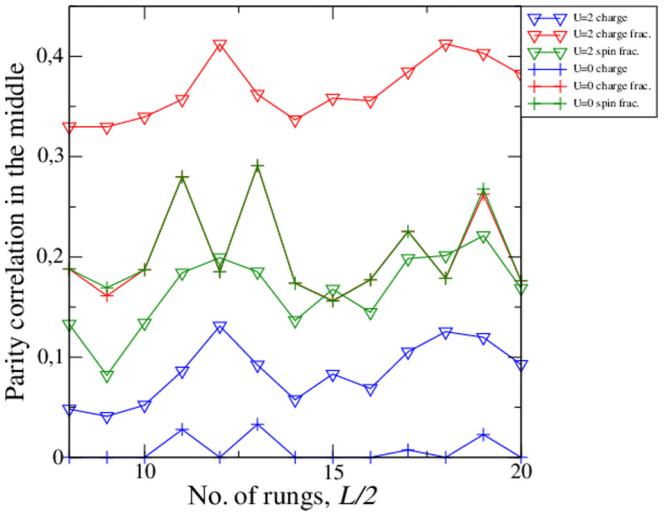

FIG. 9. Parity correlators in the middle of the ladder as functions of the total rung number $L/2$ for $U = 0$ and $U = 2$. The data for the spin fractional parity are also plotted in green. As in Fig. 3 at $U = 0$ the crosses for fractional charge and spin are almost superimposed and the nonfractional data are close to zero. At $U = 2$ the ordering of the curves is charge fractional, spin fractional, and charge nonfractional from top to bottom.

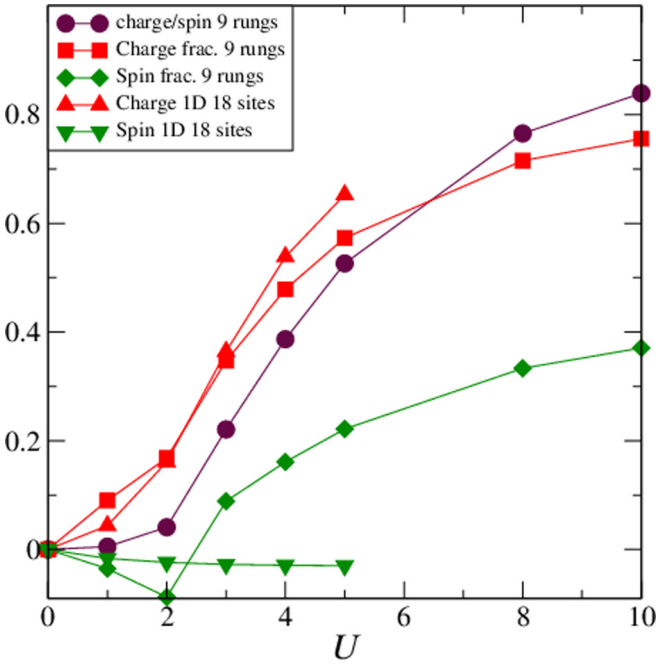

FIG. 10. Parity correlators (charge and spin, fractional and nonfractional) in the middle of the ladder as functions of U for $L = 18$ and $m_{\mathrm{DMRG}} = 2048$. Note that the nonfractional spin and charge cases on the ladder (maroon circles) coincide since $\exp(i\pi n_{j\downarrow}) = \exp(-i\pi n_{j\downarrow})$. The triangles indicate the data for a single Hubbard chain of 18 sites (see also Ref. [13]), while squares and diamonds label fractional charge and spin in the two-leg case. (Finite-size finite values at $U = 0$ have been subtracted out from the corresponding fractional data, 0.03053 for $M = 1$, 0.161 and 0.169 for $M = 2$ in charge and spin, respectively.)

value of U. If we may safely conclude that the infinite-length extrapolations are nonzero for $U \geqslant 3$, the picture again is more intricate for $U \lesssim 2$. The finite-size sequences are plotted in Fig. 9 and it is hard to decide which curve will eventually converge to a nonvanishing value for $L \to \infty$. From our data the point $U = 1$ seems to have a behavior similar to $U = 0$, but with very small or vanishing charge nonfractional order and with nonzero fractional charge and spin orders.

Finally, in order to analyze the dependence on U we consider the various parity correlators taking the rung index r in the middle of the ladder and then estimating the uniform and oscillating parts of the correlators through sum and difference of the values at r and $r - 1$. This is important because (i) we know that in the 1D case the behavior of the spin-parity for $U > 0$ is purely oscillating leading to an average vanishing asymptotic order and (ii) the decay of the parity correlators for $M = 2$ to their asymptotic values is typically nonmonotonic and in such a way we try to analyze the uniform parts in a finite-size sample at maximum distance. Already in the 1D case [13] it is seen that the maximum-distance finite-size value of parity correlators has a nonmonotonic dependence on U, so it is not easy to depict from finite-size data the behavior of the parity orders vs U. Here, with the aim of comparing the various definitions, we have conventionally subtracted out the value of each curve at $U = 0$ where the finite-size effect is expected to be larger.

The results are summarized in Fig. 10 for a choice of large $m_{\mathrm{DMRG}} = 2048$. In the depicted behavior there may be important size effects, so we have performed some additional calculations for larger system's size $L = 38$ (not plotted) and the overall trend is confirmed, even quantitatively, possibly with the exception of the region $U \lesssim 2$ (especially for the fractional spin-parity). Already in Ref. [37] it was pointed out that the DMRG calculations may not be reliable for such small values of U, because the convergence to the ground state may be poor if the number of sites is too large for the fixed threshold m_{DRMG}.

Hence we have performed additional calculations with OBC and size $L = 64$ that, from Fig. 3 in the cases examined with strongest size effects $U = 0$ and $U = 1$, is a size that seems to correspond to a sequence of local minima for the fractional orders and so it is a reasonable upper bound for the infinite-size curve. The results are reported in the last part of Sec. III B of the main text.

[1] M. den Nijs and K. Rommelse, Phys. Rev. B **40**, 4709 (1989).
[2] M. Endres *et al.*, Science **334**, 200 (2011).
[3] J. A. M. Paddison *et al.*, Science **350**, 179 (2015).
[4] X.-G. Wen, Adv. Phys. **44**, 405 (1995).
[5] A. P. Schnyder, S. Ryu, A. Furusaki, and A. W. W. Ludwig, Phys. Rev. B **78**, 195125 (2008); X. L. Qi, T. L. Hughes, and S. C. Zhang, *ibid.* **78**, 195424 (2008).
[6] F. Pollmann, A. M. Turner, E. Berg, and M. Oshikawa, Phys. Rev. B **81**, 064439 (2010).
[7] X. Chen, Z.-C. Gu, and X.-G. Wen, Phys. Rev. B **83**, 035107 (2011); **84**, 235128 (2011).
[8] A. M. Turner, F. Pollmann, and E. Berg, Phys. Rev. B **83**, 075102 (2011).
[9] B. Zeng, X. Chen, D.-L. Zhou, and X.-G. Wen, arXiv:1508.02595.
[10] F. Pollmann and A. M. Turner, Phys. Rev. B **86**, 125441 (2012).
[11] K. Duivenvoorden and T. Quella, Phys. Rev. B **86**, 235142 (2012).
[12] E. Berg, E. G. Dalla Torre, T. Giamarchi, and E. Altman, Phys. Rev. B **77**, 245119 (2008).
[13] A. Montorsi and M. Roncaglia, Phys. Rev. Lett. **109**, 236404 (2012).
[14] L. Barbiero, A. Montorsi, and M. Roncaglia, Phys. Rev. B **88**, 035109 (2013).
[15] Y. Bahri and A. Vishwanath, Phys. Rev. B **89**, 155135 (2014).
[16] F. Anfuso and A. Rosch, Phys. Rev. B **75**, 144420 (2007).
[17] F. Anfuso and A. Rosch, Phys. Rev. B **76**, 085124 (2007).
[18] S. Moudgalya and F. Pollmann, Phys. Rev. B **91**, 155128 (2015).
[19] S. P. Rath, W. Simeth, M. Endres, and W. Zwerger, Ann. Phys. (N.Y.) **334**, 256 (2013).
[20] M. Endres, Probing correlated quantum many-body systems at the single-particle level, Ph.D. thesis, LMU Munich, 2013.
[21] M. Oshikawa, J. Phys.: Condens. Matter **4**, 7469 (1992); Y. Nishiyama, N. Hatano, and M. Suzuki, J. Phys. Soc. Jpn. **65**, 560 (1996).
[22] C. N. Yang and S. C. Zhang, Mod. Phys. Lett. B **4**, 759 (1990).
[23] A. H. MacDonald, S. M. Girvin, and D. Yoshioka, Phys. Rev. B **37**, 9753 (1988).
[24] H. J. Schulz, Phys. Rev. B **53**, R2959 (1996).
[25] L. Balents and M. P. A. Fisher, Phys. Rev. B **53**, 12133 (1996).
[26] C. Wu, W. V. Liu, and E. Fradkin, Phys. Rev. B **68**, 115104 (2003).
[27] M. Tsuchiizu and A. Furusaki, Phys. Rev. B **66**, 245106 (2002).
[28] H.-H. Lin, L. Balents, and M. P. A. Fisher, Phys. Rev. B **56**, 6569 (1997).
[29] U. Ledermann, Phys. Rev. B **64**, 235102 (2001).
[30] E. Orignac and T. Giamarchi, Phys. Rev. B **56**, 7167 (1997); see also T. Giamarchi, *Quantum Physics in One Dimension* (Oxford University Press, Oxford, 2003).
[31] A. O. Gogolin, A. A. Nersesjan, and A. M. Tsvelik, *Bosonization and Strongly Correlated Systems* (Cambridge University Press, Cambridge, UK, 1998).
[32] Z. Weihong, J. Oitmaa, C. J. Hamer, and R. J. Bursill, J. Phys.: Condens. Matter **13**, 433 (2001).
[33] B. Swingle and T. Senthil, Phys. Rev. B **87**, 045123 (2013).
[34] D. Greif, M. F. Parsons, A. Mazurenko, C. S. Chiu, S. Blatt, F. Huber, G. Ji, and M. Greiner, Science **351**, 953 (2016).
[35] Y. Fuji, F. Pollmann, and M. Oshikawa, Phys. Rev. Lett. **114**, 177204 (2015).
[36] A. Juozapavičius, L. Urba, S. Caprara, and A. Rosengren, Phys. Rev. B **60**, 14771 (1999).
[37] R. M. Noack, S. R. White, and D. J. Scalapino, Physica C **270**, 281 (1996).